Inorg. Chem. **2005**, *44*, 9175–9184

Dynamic Formation of Coordination Polymers versus Tetragonal Prisms and Unexpected Magnetic Superexchange Coupling Mediated by Encapsulated Anions in the Cobalt(II) 1,3-Bis(pyrid-4-ylthio)propan-2-one Series

Benlai Wu,[†] Daqiang Yuan,[†] Benyong Lou,[†] Lei Han,[†] Caiping Liu,[†] Chunxi Zhang,*[,‡] and Maochun Hong*[,†]

State Key Laboratory of Structural Chemistry, Fujian Institute of the Research on the Structure of Matter, Chinese Academy of Sciences, Fuzhou, Fujian 350002, China, and Laboratory of Photochemistry, Center for Molecular Sciences, Institute of Chemistry, Chinese Academy of Sciences, Beijing 100080, People's Republic of China

Received March 27, 2005

The reactions of cobalt(II) halides and flexible ligand L [L = 1,3-bis(pyrid-4-ylthio)propan-2-one] under different conditions generated a series of complexes with various structural motifs ranging from tetragonal-prismatic cages to 1–3D coordination polymers. The layer diffusion of cobalt(II) chloride and L in methanol/acetone at 25 °C gave rise to a 3D polymer, $[Co(L)_2Cl_2]\cdot Me_2CO$ (**1**). At 30 °C, the slow diffusion of diethyl ether into the blue dimethylformamide (DMF) solution of complex **1** afforded a 1D polymer, $Co(L)Cl_2(DMF)_2$ (**2**). However, at 10 °C, the diffusion of diethyl ether into the DMF solution of complex **1** produced a tetragonal-prismatic cage, $[Co_2(L)_4Cl_2]Cl_2\cdot Et_2O\cdot DMF\cdot 2MeOH\cdot 4H_2O$ (**3**). The reaction of cobalt(II) bromide and L in DMF at 10 °C yielded a dimer, $[Co_2(L)_4Br_2]Br_2\cdot 6DMF\cdot 2H_2O$ (**4**), with a cage structure similar to **3**. The preparation of the series of compounds indicates the subtle relationship between structures and tunable reaction conditions. It is also found that the structural motifs vary according to the ligand conformations and that the formation of tetragonal-prismatic cages **3** and **4** may be templated by anionic guests. Magnetic studies on complexes **1**–**4** in a temperature range 4–300 K disclose that L is unfavorable for a long-range magnetic interaction; however, intramolecular spin-coupling constants of –19.6 and –21.5 cm^{-1} for **3** and **4** indicate rather strong magnetic superexchanges arising from the overlap of the d_{z^2} orbitals of the cobalt(II) and p_z orbitals of the encapsulated halide anions. Electron paramagnetic resonance (EPR) spectra of complexes **3** and **4** in solution and solid give information that both complexes are high-spin cobalt(II) compounds with a rhombic distortion of the axial zero-field splitting. Interestingly, the intramolecular magnetic-exchange coupling in **3** and **4** mediated by the encapsulated anion Cl^- or Br^- is also reflected by the EPR spectra.

Introduction

Coordination networks and metallacages receive intense current attention because of their structurally esthetical appeal and potential for molecular materials with technologically applicable properties.[1] Self-assembly through coordinate bond formation between metal ions and bridging ligands is now a widespread method for obtaining both coordination polymers and cages. On the basis of this method, a series of ingenious synthetic strategies, such as the "Molecular Library Model", "Symmetry Interaction Model",[2] and "Reticular

* To whom correspondence should be addressed. E-mail: hmc@ms.fjirsm.ac.cn (M.H.). Fax: +86-591-83714946 (M.H.).

† State Key Laboratory of Structural Chemistry, Fujian Institute of the Research on the Structure of Matter, Chinese Academy of Sciences.

‡ Laboratory of Photochemistry, Center for Molecular Sciences, Institute of Chemistry, Chinese Academy of Sciences.

(1) (a) Müler, I. M.; Spillmann, S.; Franck, H.; Pietschnig, R. *Chem.—Eur. J.* **2004**, *10*, 2207. (b) Kuehl, C. J.; Huang, S. D.; Stang, P. J. *J. Am. Chem. Soc.* **2001**, *123*, 9634. (c) Hamiton, T. D.; MacGillivray, L. R. *Cryst. Growth Des.* **2004**, *4*, 419. (d) Batten, S. R.; Robson, R. *Angew. Chem., Int. Ed.* **1998**, *37*, 1460. (e) Kim, J.; Chen, B.; Reineke, T. M.; Li, H.; Eddaoudi, M.; Moler, D. B.; O'Keeffe, M.; Yaghi, O. M. *J. Am. Chem. Soc.* **2001**, *123*, 8239. (f) Huang, X.-C.; Zhang, J.-P.; Lin, Y.-Y.; Yua, X.-L.; Chen, X.-M. *Chem. Commun.* **2004**, 1100. (g) Yoshida, N.; Ichikawa, K. *Chem. Commun.* **1997**, 1091.

10.1021/ic050455v CCC: $30.25 © 2005 American Chemical Society
Published on Web 11/03/2005

Synthesis",[3] have been well established for the design of new structures. Besides the spontaneous metal/ligand association, the organization of such compounds is also impacted by noncovalent interactions, which offer a rich scope for the modification of the outcome. One important example in this aspect is guest templation (involving neutral, cationic and anionic, and even complex guests), which has scored some success in the generation of metallaassemblies recently.[4] Thus far, product prediction is still limited by the dynamic nature endowed in metal-mediated self-assembly reactions, where the kinetic formation of metal−ligand bonds, the varying coordination number and stereochemistry of metal ions, and the coordination modes of ligands may increase the lability in metal complexes.[5] Additionally, the diversity of assemblies in structures and further in properties may result from other factors such as the metal/ligand ratio, solvents, counterions, and even temperature. For instance, Pan et al. reported solvent-dependent reversible transformations of nano- and nonporous coordination frameworks.[6] Armentano et al. showed that the magnetic ordering temperature T_c varies with cations in oxo- and oxalate-bridged 3D iron(II) networks.[7]

One conspicuous way to fascinating metallaassemblies, such as well-defined metal-containing cages, helicates, and interpenetrating or dynamic porous frameworks, is the use of flexible or semiflexible organic linkers.[8,9] Particularly, the flexibility of entities endows assembly systems with the propensity toward structural diversity, which affords opportunities to probe how the self-assembly process is adjusted by modifying the reaction conditions.[10] The chemistry reported here is based on the flexible ditopic ligand 1,3-bis(pyrid-4-ylthio)propan-2-one (L), shown in Chart 1. Also shown are its multiple conformational isomers. Relating to the rigid plane of the propan-2-one group, its ether linkage offers the possibility of cis or trans orientations of the side arms, accompanied with the two binding sites pointing in the same or reverse directions.[11] Thus, it is an attractive candidate for use in the generation of both molecular cages and coordination polymers. Cobalt(II) ions with labile coordination configurations and interesting magnetism are purposely selected as binding nodes for self-assembly reactions with L.[12] With changes in the reaction conditions such as the solvents, counterions, and temperature, a series of cobalt(II) halide complexes of the composition $[Co(L)_nX_2]$ ($n = 1$ or 2, $X = Cl^-$ and Br^-) have been obtained, which exhibit markedly different structures ranging from molecular cages to 1−3D coordination polymers. Very interestingly, there is a dynamic formation of the cage and polymers in cobalt(II) chloride−L complexes, showing solvent-assisted structural conversion in response to the temperature. Remarkably, the structural switching from coordination polymers to cages is concomitant with a considerable change in the conformation of ligand L.

Chart 1. Schematic Representation of the Conformational Isomers of Ligand L

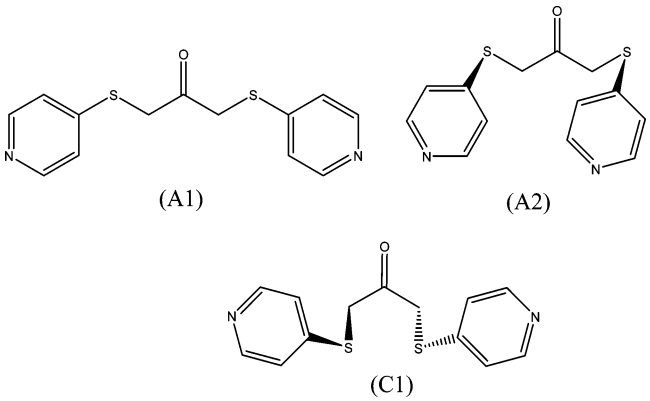

Magnetostructural correlations have been studied extensively in recent years.[13] However, in the host−guest chemistry of metal-containing cages, the magnetic properties of hosts affected by guests, which perhaps relates to the utmost understanding of magnetic transmission in organisms, have rarely been reported. We also report the magnetic studies

(2) (a) Leininger, S.; Olenyuk, B.; Stang, P. J. *Chem. Rev.* **2000**, *100*, 853. (b) Stang, P. J. *Chem.—Eur. J.* **1998**, *4*, 19. (c) Holliday, B. J.; Mirkin, C. A. *Angew. Chem., Int. Ed.* **2001**, *40*, 2023. (d) Fujita, M.; Umemoto, K.; Yoshizawa, M.; Fujita, N.; Kusukawa, T.; Biradha, K. *Chem. Commun.* **2001**, 509.

(3) (a) Yaghi, O. M.; O'Keeffe, M.; Ockwig, N. W.; Chae, H. K.; Eddaoudi, M.; Kim, J. *Nature* **2003**, *423*, 705. (b) Eddaoudi, M.; Kim, J.; Rosi, N.; Vodak, D.; Wachter, J.; O'Keeffe, M.; Yaghi, O. M. *Science* **2002**, *295*, 465.

(4) (a) Anderson, S.; Anderson, H. L.; Sanders, J. K. M. *Acc. Chem. Res.* **1993**, *26*, 469. (b) Raehm, L.; Mimassi, L.; Guyard-Duhayon, C.; Amouri, H. *Inorg. Chem.* **2003**, *42*, 5654. (c) Diaz, P.; Mingos, D. M. P.; Vilar, R.; White, A. J. P.; Williams, D. J. *Inorg. Chem.* **2004**, *43*, 7597. (d) Yue, N. L. S.; Eisler, D. J.; Jennings, M. C.; Puddephatt, R. J. *Inorg. Chem.* **2004**, *43*, 7671. (e) Zhou, Y.-F.; Jiang, F.-L.; Yuan, D.-Q.; Wu, B.-L.; Wang, R.-H.; Lin, Z.-Z.; Hong, M.-C. *Angew. Chem., Int. Ed.* **2004**, *43*, 5665.

(5) (a) Burchell, T. J.; Eisler, D. J.; Puddephatt, R. J. *Inorg. Chem.* **2004**, *43*, 5550. (b) Bi, W.; Cao, R.; Sun, D.; Yuan, D.; Li, X.; Wang, Y.; Li, X.; Hong, M. *Chem. Commun.* **2004**, 2104. (c) Yoshida, N.; Oshio, H.; Ito, T. *Chem. Commun.* **1998**, 63.

(6) Pan, L.; Liu, H.; Lei, X.; Huang, X.; Olson, D. H.; Turro, N. J.; Li, J. *Angew. Chem., Int. Ed.* **2003**, *42*, 542.

(7) Armentano, D.; Munno, G. D.; Mastropietro, T. F.; Proserpio, D. M.; Julve, M.; Lloret, F. *Inorg. Chem.* **2004**, *43*, 5177.

(8) (a) Fleming, J. S.; Mann, K. L. V.; Carraz, C.; Psillakis, E.; Jeffery, J. C.; McCleverty, J. A.; Ward, M. D. *Angew. Chem., Int. Ed.* **1998**, *37*, 1279.(b) Fujita, M.; Nagao, S.; Ogura, K. *J. Am. Chem. Soc.* **1995**, *117*, 1649.

(9) (a) Seo, J. S.; Whang, D.; Lee, H.; Jun, S. I.; Oh, J.; Jeon, Y. J.; Kim, K. *Nature* **2000**, *404*, 982. (b) Hong, M.-C.; Su, W.-P.; Cao, R.; Fujita, M.; Lu, J.-X. *Chem.—Eur. J.* **2000**, *6*, 427. (c) Bu, X.-H.; Chen, W.; Lu, S.-L.; Zhang, R.-H.; Liao, D.-Z.; Bu, W.-M.; Shionoya, M.; Brisse, F.; Ribas, J. *Angew. Chem., Int. Ed.* **2001**, *40*, 3201. (d) Uemura, K.; Kitagawa, S.; Kondo, M.; Fukui, K.; Kitaura, R.; Chang, H.-C.; Mizutani, T. *Chem.—Eur. J.* **2002**, *8*, 3586. (e) Pan, L.; Adams, K. M.; Hernandez, H. E.; Wang, X.; Zhang, C.; Hattori, Y.; Kaneko, K. *J. Am. Chem. Soc.* **2003**, *125*, 3062. (f) Kondo, M.; Irie, Y.; Shimizu, Y.; Miyazawa, M.; Kawaguchi, H.; Nakamura, A.; Naito, T.; Maeda, K.; Uchida, F. *Inorg. Chem.* **2004**, *43*, 6139.

(10) (a) Carlucci, L.; Ciani, G.; Macchi, P.; Proserpio, D. M.; Rizzato, S. *Chem.—Eur. J.* **1999**, *5*, 237. (b) Reger, D. L.; Semeniuc, R. F.; Rassolov, V.; Smith, M. D. *Inorg. Chem.* **2004**, *43*, 537. (c) Cordes, D. B.; Bailey, A. S.; Caradoc-Davies, P. L.; Gregory, D. H.; Hanton, L. R.; Lee, K.; Spicer, M. D. *Inorg. Chem.* **2005**, *44*, 2544.

(11) Wu, B.; Yuan, D.; Jiang, F.; Han, L.; Lou, B.; Liu, C.; Hong, M. *Eur. J. Inorg. Chem.* **2005**, 1303.

(12) (a) Heinze, K.; Hutter, G.; Zsolnai, L.; Schober, P. *Inorg. Chem.* **1997**, *36*, 5457. (b) Hayami, S.; Hashiguchi, K.; Juhász, G.; Ohba, M.; Ohkawa, H.; Maeda, Y.; Kato, K.; Osaka, K.; Takata, M.; Inoue, K. *Inorg. Chem.* **2004**, *43*, 4124. (c) Tong, M.-L.; Kitagawa, S.; Chang, H.-C.; Ohba, M. *Chem. Commun.* **2004**, 418. (d) Gutschke, S. O. H.; Price, D. J.; Powell, A. K.; Wood, P. T. *Angew. Chem., Int. Ed.* **2001**, *40*, 1920.

(13) (a) Thompson, L. K.; Mandal, S. K.; Tandon, S. S.; Bridson, J. N.; Park, M. K. *Inorg. Chem.* **1996**, *35*, 3117. (b) Suzuki, Y.; Fujimori, M.; Yoshikawa, H.; Awaga, K. *Chem.—Eur. J.* **2004**, *10*, 5158. (c) Lambert, S. L.; Hendrickson, D. N. *Inorg. Chem.* **1979**, *18*, 2683.

on the cages of cobalt(II) halides and 1,3-bis(pyrid-4-ylthio)-propan-2-one, which show unexpectedly strong antiferromagnetic interactions mediated by the encapsulated anions Cl^- and Br^-, respectively. Of particular interest is that they are rare models in which the magnetic exchange of binuclear Co(II) is dominated by the weak interactions of the encapsulated anion and two metal centers. Compared with all reported magnetism in halide-bridged binuclear complexes, the above observation probably provides an atypical case that furthers the understanding of magnetic-superexchange coupling.[14]

Results and Discussion

1. Synthesis and Solution Structure Study. Ligand L was prepared using our previously reported method.[11] As mentioned above, ligand L displays multiple conformational isomers in building metal-containing complexes. The typical isomers presented in this paper are A1, A2, and C1 isomers. With their two binding sites pointing in reverse directions, A1 and C1 isomers show a preference for constructing open frameworks. However, the A2 isomer with its binding sites pointing in the same direction, like a molecule clip, tends to create metallacycles or cages.

At 25 °C, the layer diffusion of cobalt(II) chloride and L in a mole ratio of 1:2 in methanol/acetone gave rise to a suspended blue-green substance in about 5 min, which altered into orange crystals of a 3D polymer, $[Co(L)_2Cl_2]\cdot Me_2CO$ (**1**), in another 5 min. At 30 °C, the slow diffusion of diethyl ether into the blue dimethylformamide (DMF) solution of freshly prepared complex **1** for 2 weeks created single-phase red prismatic crystals of a 1D polymer, $Co(L)Cl_2(DMF)_2$ (**2**). However, at a lower temperature of 10 °C, the diffusion process first created green jelly, which then changed into purple prismatic crystals of a dimeric cage, $[Co_2(L)_4Cl_2]Cl_2\cdot Et_2O\cdot DMF\cdot 2MeOH\cdot 4H_2O$ (**3**), in 3 weeks. At 30 °C, the slow diffusion of diethyl ether into a blue DMF solution of **3** again produced complex **2** in 2 weeks. To further explore anionic effects upon structural topologies, cobalt(II) bromide was used to assemble with L in DMF. Unfortunately, only purple prismatic crystals of a dimer, $[Co_2(L)_4Br_2]Br_2\cdot 6DMF\cdot 2H_2O$ (**4**), with a cagelike structure similar to that of **3** were obtained at 10 °C.

The preparation of cobalt(II) chloride−L compounds, which is represented in Scheme 1, suggests a dynamic formation process in response to changes in the solvents and temperature. The formation of such different structures through the self-assembly of L with the same metal ion warrants further electrospray ionization mass spectrometry (ESI-MS) studies on the solution behavior of complexes **1**, **3**, and **4**. The ESI-MS spectral data are given in Table 1, where the main ions characteristic of complexes present in solution are listed. Every ion is verified by careful comparison of the isotopic patterns between the observed peak and the theoretical simulation. The common feature in the spectra of complexes **1**, **3**, and **4** is that all display the strong peak relating to free ligand L and the minor peaks corresponding to hydrogen-bonding adducts $L\cdot 2H_2O$ for **1** and $L\cdot 2MeOH$ for **3** and **4**. The spectrum of **1** in DMF gives major peaks corresponding to $[CoCl(DMF)_3]^+$, $[CoCl_2(DMF)_3]$, $[Co_2Cl_3(L)_2]^+$, and $[Co_2Cl_2(L)_4]^{2+}$, evidently indicating the formation of tetragonal-prismatic dication $[Co_2Cl_2(L)_4]^{2+}$. Indeed, the ESI-MS spectrum of **1** in DMF does not really represent that of itself. As dissolved in DMF, the network of **1** may be decomposed into multiple species involving free ligand L, major mono- and binuclear complexes, and possible oligomers. Presumably, there is an equilibrium between various molecular fragments of **1** formed when DMF coordinates to it, and with diffusion of diethyl ether into the system, the coordination sites held by DMF will be substituted by ligands L, which can bridge cobalt(II) ions to form new temperature-dependent compounds: polymer **2** at higher temperature and dimeric cage **3** at lower temperature. The spectra of **3** and **4** in methanol dominated by a series of peaks corresponding to dinuclear cations $[Co_2X_3(L)_2]^+$, $[Co_2X_2(L)_2(H_2O)_2]^{2+}$, $[Co_2X_2(L)_2(MeOH)_2]^{2+}$, and $[Co_2X_2(L)_4]^{2+}$, respectively ($X = Cl^-$ for **3** and Br^- for **4**), suggest that there may be a fast exchange between L and solvents in solution and that the tetragonal-prismatic dications $[Co_2X_2(L)_4]^{2+}$ are the preferable members in the equilibrium systems because of the compared higher peaks attributed to them in the spectra (Figure S1 in the Supporting Information).

Scheme 1. Schematic Representation of the Dynamic Formation of Cobalt(II) Chloride−L Complexes in Response to Changes in the Solvent Systems and Temperature

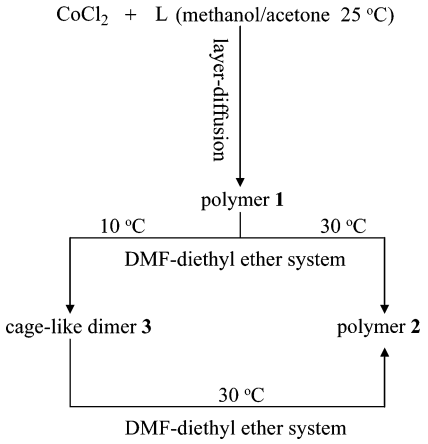

The solution features of cages **3** and **4** were also investigated by spectrophotometric measurements. Because of their insolubility or slight solubility in common solvents, the UV−vis spectrum records in the visible light area for cages **3** and **4** might be limited. Both **3** and **4** in a methanol solution show a salient absorption maximum at 261 nm with a shoulder at 337 nm for **3** and 335 nm for **4** observed at a higher concentration of about $\sim 10^{-4}$ M. Spectrophotometric titrations were performed by the addition of $CoCl_2$ or $CoBr_2$

(14) (a) Sakiyama, H.; Ito, R.; Kumagai, H.; Inoue, K.; Sakamoto, M.; Nishida, Y.; Yamasaki, M. *Eur. J. Inorg. Chem.* **2001**, 2027. (b) Sun, J.-S.; Zhao, H.; Ouyang, X.; Clérac, R.; Smith, J. A.; Clemente-Juan, J. M.; Gómez-Garcia, C.; Coronado, E.; Dunbar, K. R. *Inorg. Chem.* **1999**, *38*, 5841. (c) Telfer, S. G.; Sato, T.; Kuroda, R.; Lefebvre, J.; Leznoff, D. B. *Inorg. Chem.* **2004**, *43*, 421. (d) Grove, H.; Kelly, T. L.; Thompson, L. K.; Zhao, L.; Xu, Z.; Abedin, T. S. M.; Miller, D. O.; Goeta, A. E.; Wilson, C.; Howard, J. A. K. *Inorg. Chem.* **2004**, *43*, 4278. (e) Seeber, G.; Kögerler, P.; Kariuki, B. M.; Cronin, L. *Chem. Commun.* **2004**, 1580.

Table 1. ESI-MS Data[a] for **1**, **3**, and **4**

compd	characteristic ions (neutral complexes with added H^+)
1[b]	$[Co(DMF)_3Cl]^+$ 313.1 (313.1); $[Co(DMF)_3Cl_2]$ 349.8 (350.1); $[Co_2(L)_4Cl_2]^{2+}$ 645.9 (646.0); $[Co_2(L)_2Cl_3]^+$ 776.8 (777.0)
3[c]	$[Co_2(L)_2(H_2O)_2Cl_2]^{2+}$ 388.1 (388.0); $[Co_2(L)_2(MeOH)_2Cl_2]^{2+}$ 401.9 (402.0); $[Co_2(L)_4Cl_2]^{2+}$ 646.0 (646.0); $[Co_2(L)_2Cl_3]^+$ 776.9 (777.0)
4[c]	$[Co_2(L)_2(H_2O)_2Br_2]^{2+}$ 431.9 (431.9); $[Co_2(L)_2(MeOH)_2Br_2]^{2+}$ 448.0 (447.3); $[Co_2(L)_4Br_2]^{2+}$ 692.0 (691.6); $[Co_2(L)_2Br_3]^+$ 910.6 (910.3)

[a] *m*/*z* values are given for the highest isotope line in Da and theoretical values in parentheses. [b] In DMF. [c] In MeOH.

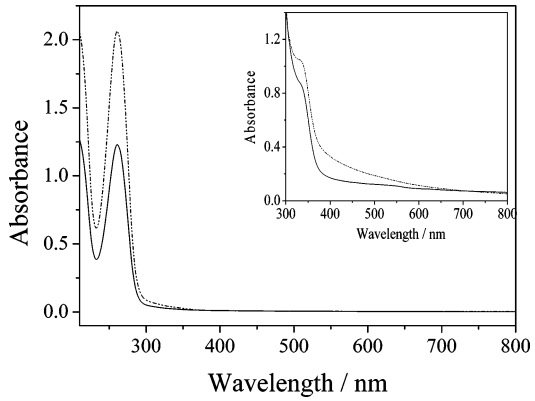

Figure 1. UV−vis spectra of complexes **3** (solid line) and **4** (dash-dot-dotted line) in methanol with the concentrations of 2.0×10^{-5} and 3.5×10^{-4} M (inset).

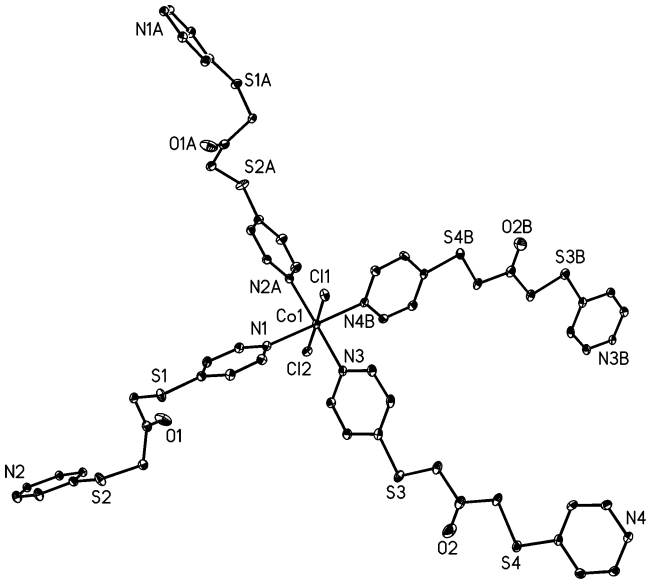

Figure 2. ORTEP representation of a pseudo-C_2-symmetric array of two-sorted conformational isomers A1 and C1 around six-coordinated Co(II) centers in complex **1** (30% thermal ellipsoids; hydrogen atoms omitted for clarity).

to a solution of L in methanol. The results show that the absorption intensity at 261 nm decreases, whereas that of the broad absorptions at 337 nm for **3** and 335 nm for **4** increases with the addition of Co(II) up to a Co/L ratio of 1:2 (Figure S2 in the Supporting Information). In conjugation with the UV−vis spectrum of L in methanol, the high-energy absorption bands at 261 nm can be attributed to the absorption of ligand L, while the low-energy absorption shoulders around 337 nm for **3** and 335 nm for **4** perhaps relate to the absorption of the cages (Figure 1).

In summary, the preparation of **1**−**4** is sensitive to the reaction conditions, which is demonstrated by the dynamic formation of the cobalt(II) chloride−L complexes in response to changes in the solvents and temperature. Solution studies show that the dimeric cages can exist in solution as considerably stable species.

2. Crystal Structure of 1. Complex **1** displays a 3D 6-fold-interpenetrating diamondoid framework. The asymmetric unit consists of a cobalt(II) chloride unit, two L's, and an acetone molecule. Each square-planar node Co(II) linked by four L's is in a distorted octahedral environment surrounded by four pyridyls occupying the equatorial sites in a paddlewheel manner and two Cl^- ions occupying the axial sites (Figure 2). The bond distances range from 2.180(3) to 2.186(3) Å for Co−N and from 2.4106(12) to 2.4283(12) Å for Co−Cl, and the in-plane and axis-transition angles are 178.76(12), 178.82(12), and 178.98(4)°, respectively. The exo-bidentate spacers L in **1** display the A1 and C1 conformations, which pack in the A1A1C1C1 form around metal centers. As a result, a pseudo-C_2 axis passes through their Co(II) center and equally bisects their equatorial plane. Furthermore, neighboring L's around each Co(II) center extend above or below the equatorial plane, which results in the sharp deviations of the other four binding sites of L from the least-squares plane. It can be clearly expected that four metal nodes bonded to the four nitrogen atoms will be located at the vertexes of a distorted tetrahedron. Thus, in this manner, a 3D diamondoid framework forms (Figure 3a). The separations of the adjacent Co(II)···Co(II) bridged by A1 and C1 are 16.677 and 14.992 Å, respectively. The complex adopts a 6-fold interpenetration to fill large cavities within the diamondoid cages (Figure 3b). Nevertheless, acetone molecules are included in their porous frameworks.

3. Crystal Structure of 2. Complex **2** has a 1D chain architecture in which every cobalt(II) ion located at the inversion center *i* reproduces the whole molecule through the asymmetry unit consisting of half cobalt(II) chloride unit, half L, and one DMF molecule. As shown in Figure 4, the Co(II) node, which is ligated by two oxygen atoms of DMF, two nitrogen atoms from different L units in the equatorial plane, and two Cl^- ions at the axial sites, adopts an axially elongated octahedral geometry with Co−N, Co−O, and Co−Cl bond distances at 2.1932(15), 2.1421(13), and 2.4407(5) Å, respectively, and the in-plane and axis-transition angles all at 180.0°. The bond distances of Co−N and Co−Cl in complex **2** are slightly longer than those in complex **1**, and ligands L in complex **2** only present A1 isomers to bind metal nodes with the separation distance of 16.265 Å, being slight shorter than that found in **1**. Although complex **2** is derived from complex **1**, the two have substantial differences in

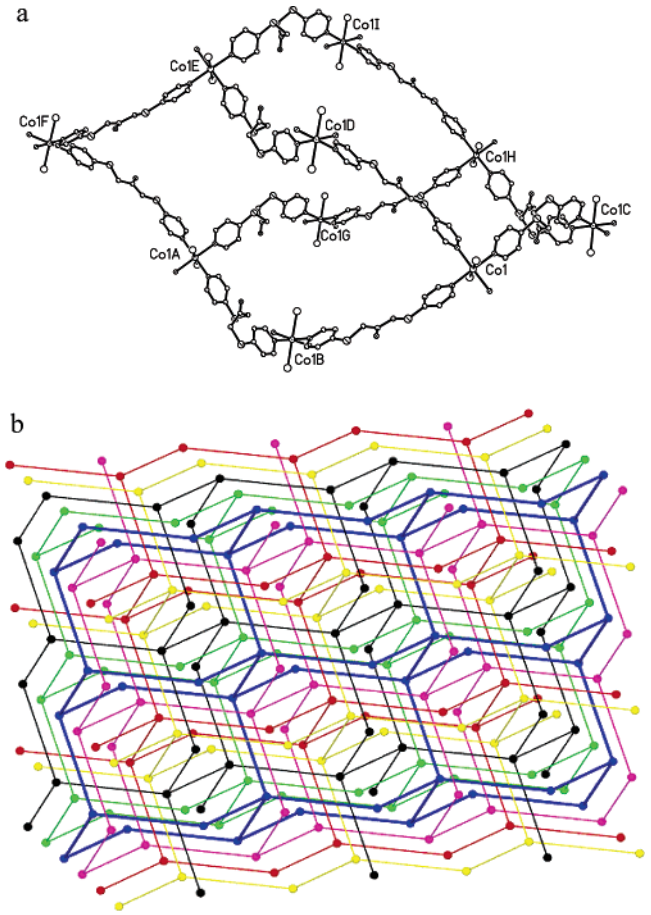

Figure 3. View of a diamondoid cage unit generated through 12 L (6 A1 and 6 C1) bridging 10 Co(II) centers (a) and a 6-fold-interpenetrating diamondoid network with bridging and terminal ligands L and Cl^- omitted for clarity (b) in **1**.

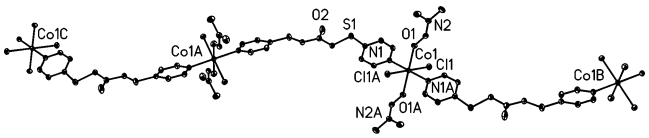

Figure 4. ORTEP representation of a 1D chain structure connected only by A1 isomers in complex **2** (30% thermal ellipsoids; hydrogen atoms omitted for clarity).

structure. Clearly, the main cause for the conversion of complex **1** into **2** is the solvent system. In a methanol/acetone medium, the fast assembly of $CoCl_2$ and L tends to produce the 3D diamondoid framework **1**, whereas the stronger polar solvent DMF not only decomposes **1** but also takes part in coordination with metal centers, thereby limiting structural extension and finally resulting in the 1D chain polymer **2**.

4. Crystal Structures of 3 and 4. In contrast to polymers **1** and **2**, complexes **3** and **4** are discrete aggregates. As shown in Figure 5, four L molecules with the typical cliplike conformation A2 bond two square-planar nodes Co(II) in the equatorial plane to build a basic cage unit, and one halide anion (Cl^- for **3** and Br^- for **4**) ligates to every Co(II) node at the apical position to complete a distorted square-pyramidal coordination symmetry. Consequently, slightly deviated tetragonal-prismatic dications $[Co_2(L)_4X_2]^{2+}$ form. In **3**, all Co−N distances fall in the range from 2.140(5) to 2.159(5) Å, being close to those in **4** [from 2.137(2) to 2.159-

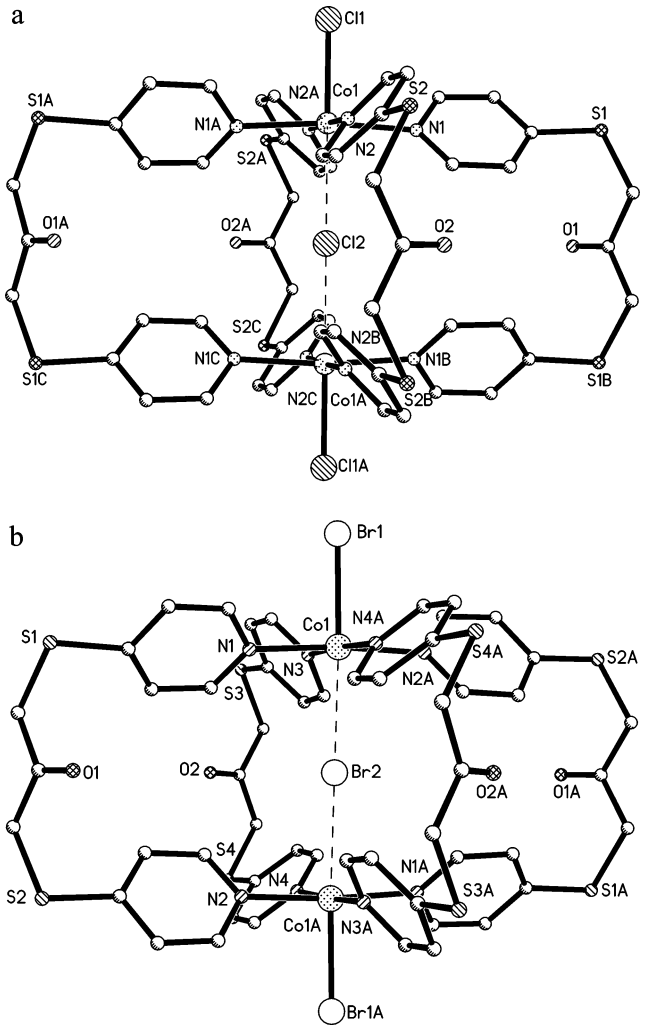

Figure 5. Ball-and-stick representation of the prismatic cages generated by four A2 isomers connecting binuclear cobalt(II), showing encapsulated anions Cl^- in **3** (a) and Br^- in **4** (b).

(2) Å]. The Co−N distances in both **3** and **4** are somewhat shorter than those found in polymers **1** and **2**. The Co−Cl and Co−Br distances are 2.424(3) and 2.6046(4) Å for **3** and **4**, respectively. In comparison with the reported dimeric tetragonal prisms,[15] the tetragonal prisms in **3** and **4** display a lower symmetry. In the prismatic dication $[Co_2(L)_4Cl_2]^{2+}$ of **3**, a mirror plane *m* containing the propan-2-one groups of L divides the dication into two equivalent parts, and a C_2 axis passes through the two Co(II) ions. Thus, the prismatic dication possesses C_{2h} symmetry. In the analogue prismatic dication $[Co_2(L)_4Br_2]^{2+}$, ligand L merely possesses C_1 symmetry and only an inversion center *i* is located at the center of the cluster. However, four ligands L are arranged in such a way that C_{4h} symmetry could be imagined to impose on the tetragonal prisms. The deviation from a highly symmetric tetragonal prism is probably due to the symmetry lowering of L and the coordination geometry around metal nodes.

Complexes **3** and **4** show very similar packing motifs, clearly presented in Figure 6. The dicationic prisms stack in

(15) (a) Barbour, L. J.; Orr, G. W.; Atwood, J. L. *Nature* **1998**, *393*, 671. (b) Su, C.-Y.; Cai, Y.-P.; Chen, C.-L.; Smith, M. D.; Kaim, W.; zur Loye, H.-C. *J. Am. Chem. Soc.* **2003**, *125*, 8595.

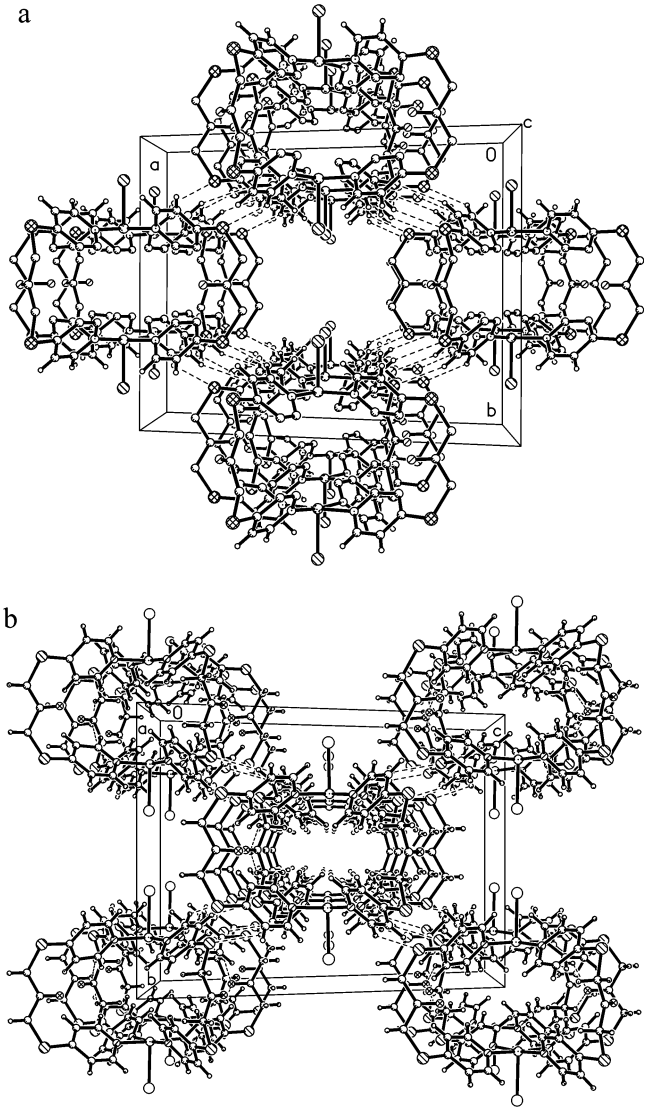

Figure 6. Parallel arrangements of tetragonal prisms linked by weak (pyridyl)C−H···S hydrogen bonding to create large channels in **3** (a) and **4** (b) (guest solvents, encapsulated anions, and partial hydrogen atoms omitted for clarity).

linear arrays with their Co(II)···Co(II) axes parallel to [010], and each array is bridged by four identical nearest-neighbor arrays with weak (pyridyl)C−H···S hydrogen bonding. As a result, large channels that host a number of solvent guest molecules form. Interestingly, the linear arrangements along the *c* axis for **3** and the *a* axis for **4** are reinforced by complicated weak interactions. As depicted in Figure 7, free anion X binds adjacent prismatic cations together through four C−H···X hydrogen bonds formed with propan-2-one groups (C···Cl, 3.608 Å; C···Br, 3.665 or 3.693 Å) and two O−H···X hydrogen bonds formed with water molecules O6 (O···Cl, 3.164 Å; O···Br, 3.327 Å). Thus, 6-fold hydrogen bonding to every acceptor X is formed. Moreover, the water molecule O6 ligates to O2 in the propan-2-one groups through an O−H···O hydrogen bond (O···O distances of 2.994 and 2.966 Å for **3** and **4**, respectively), and the O2 atom further links to the adjacent propan-2-one groups through two C−H···O hydrogen bonds with C···O distances of 3.319 Å for **3** and 3.222 and 3.365 Å for **4**.

The most interesting structural feature in complexes **3** and **4** is that each dicationic cage at its structural center encapsulates a halogen guest anion that weakly interacts with two Co(II) nodes. The separation of two Co(II) ions bridged by L in **3** is 5.636 Å and thus the distance between the metal node and accommodated Cl^- is 2.818 Å, and those in **4** are 5.807 and 2.904 Å, respectively. Through weak interactions with Co(II), the encapsulated anions Cl^- and Br^- may template the formation of $Co_2(L)_4$ prisms by stabilizing this structural motif in crystallization.

As observed by the crystallographic data, the conformations of L may manipulate the structural motifs in the series of cobalt(II) halide−L complexes. The combination of cobalt(II) and L in A1 and C1 isomers creates coordination polymer **1** or **2**, whereas the assemblies of L in the A2 conformation are cages **3** and **4**. Additionally, the transformation of complex **1** into complex **3** is obviously accompanied with a conformational change of ligand L from the A1 and C1 isomers in **1** to the A2 isomer in **3**, which is easily carried out in solution because of the lower steric energies of about 5−22 kJ/mol calculated by Gaussian03 among the isomers.[11]

5. Electron Paramagnetic Resonance (EPR) Spectra of Complexes 3 and 4. Figure 8 shows the EPR spectra of complexes **3** and **4** in methanol and polycrystalline powders. Complexes **3** and **4** in methanol have almost the same EPR centered at $g_\perp \approx 4.4$ and $g_{||} = 2.3$. However, polycrystalline powders of **3** and **4** give EPR spectra dramatically different from those observed in methanol. The spectrum of **3** comprises a broad derivative centered at $g_\perp = 4.2$ and a negative feature centered at $g_{||} = 2.9$, while that of complex **4** consists of a broad derivative centered at $g_\perp = 5.2$ and a negative feature centered at $g_{||} = 3.1$. The EPR spectra of **3** and **4** in both solution and solid exhibit a $S = {}^3/_2$ signal with observed anisotropic *g* values, indicating a typical high-spin cobalt(II) complex with a rhombic distortion of the axial zero-field splitting.[16] In methanol, the encapsulated anions X in dimeric cages (Cl^- for **3** and Br^- for **4**) are strongly solvated, and the bridging anions (Cl^- or Br^-) between two Co(II) ions would be replaced by solvent molecules. Consequently, similar EPR spectra are observed for complexes **3** and **4** in glassy methanol samples. In polycrystalline powders, the different bridged anions between two Co(II) centers give rise to the different magnetic-exchange coupling between two metal ions in complexes **3** and **4**, respectively, leading to the obvious distinction in their EPR spectra. The comparatively bigger change in the EPR spectrum of polycrystalline sample **4** to those of glassy methanol samples indicates stronger dinuclear coupling mediated by the encapsulated Br^-.

6. Magnetic Properties of Complexes 3 and 4. The temperature-dependent magnetic susceptibility (χ_M) of polycrystalline samples **3** and **4** was measured in the temperature range 4−300 K, and the corresponding graphs of χ_M vs *T* and μ_{eff} (magnetic moment per cobalt atom) vs *T* are shown

(16) Banci, L.; Benelli, C.; Gatteschi, D.; Zanchini, C. *Struct. Bonding (Berlin)* **1982**, *52*, 37.

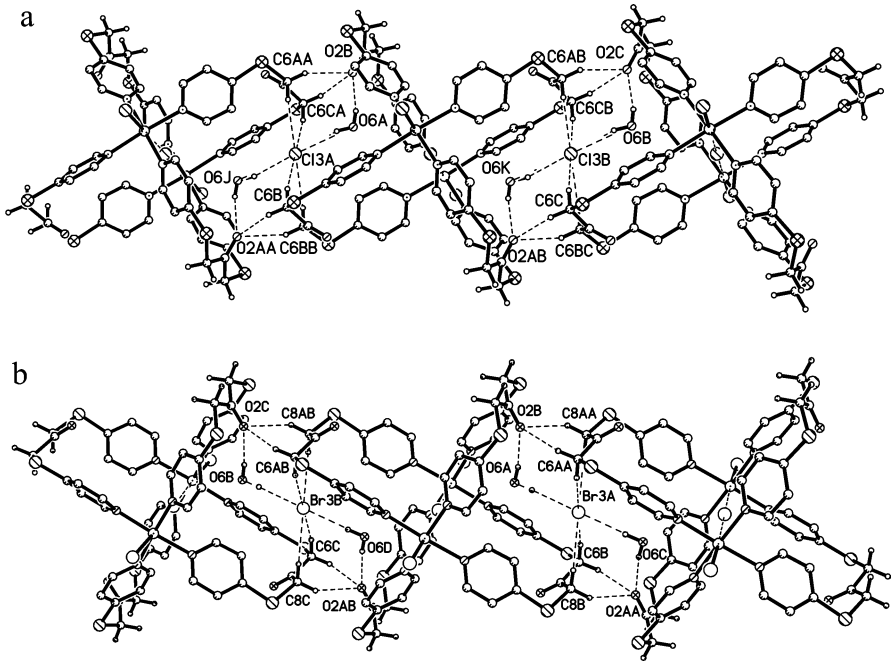

Figure 7. 1D polycages connected by complicated hydrogen bonds of C−H···X, O−H···X, O−H···O, and C−H···O in **3** (a) and **4** (b) (X = Cl^- for **3** and Br^- for **4**).

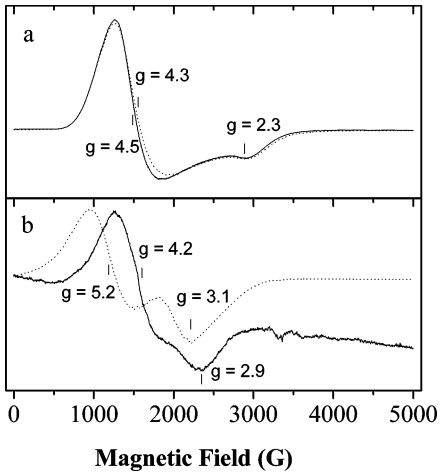

Figure 8. (a) EPR spectra of glassy methanol solutions of complexes **3** (solid line) and **4** (dotted line). (b) EPR spectra of polycrystalline powders of complexes **3** (solid line) and **4** (dotted line). Conditions of measurement: temperature, 6 K; microwave power, 1 mW; modulation amplitude, 10 G; microwave frequency, 9.38 GHz.

in parts a and b of Figure 9, respectively. These data suggest the presence of strong antiferromagnetic-exchange interactions in the $S_1 = S_2 = {}^3/_2$ binuclear cobalt(II) complexes. For **3**, there is a rounded maximum at 45 K in the χ_M curve and its μ_{eff} value decreases continuously with temperature from 4.30 μ_B at 300 K to 1.05 μ_B at 4 K. For **4**, a similar maximum in the χ_M curve occurs at 56 K, with its μ_{eff} value continuously decreasing with temperature from 4.47 μ_B at 300 K to 0.79 μ_B at 4 K. The μ_{eff} values of both complexes at room temperature are larger than the spin-only magnetic moment expected for three unpaired electrons (3.87 μ_B), indicating a high-spin d^7 configuration with the modest orbital contribution. Thus far, quantitative magnetic analyses of cobalt(II) complexes have been a challenge because of the complexity of magnetic anisotropy originating from the

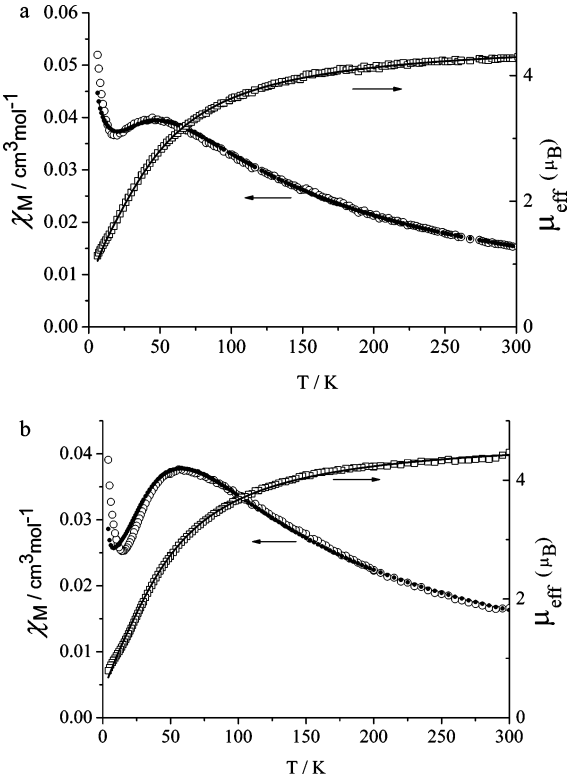

Figure 9. χ_M (○) vs T plot with the theoretical fit (●) and μ_{eff} (□) vs T plot with the theoretical fit (—) for **3** (a) and **4** (b).

spin−orbit coupling and axial distortion. The isotropic model for these binuclear cobalt(II) compounds proves to be unsuccessful in fitting the magnetic data, which can be understood with reference to their structural features and EPR results. The cobalt(II) centers in complexes **3** and **4** are located in a distorted square-pyramidal ligand field N_4X or a more distorted octahedral ligand field N_4X_2 (in consideration of the additional pseudocoordination from the encap-

sulated halide ion), and these sharp deviations at the axis would lead to markedly magnetic anisotropy and axial zero-field splitting. In addition, the complicated weak interactions among prismatic dications would have a certain effect on the magnetic behavior, which needs further consideration for the molecular field approximation. The Curie tails observed below 17 K for **3** and 13 K for **4** are attributed to a small amount of $S = {}^3/_2$ paramagnetic impurity. In this context, we use the software package MAGMUN4.0 to factor in the exchange interaction J, the average g, the axial zero-field splitting parameter D, the Weiss-like constant Θ, and the ρ parameter denoting the molar fraction of a magnetically dilute impurity, and this modeling reproduces the experimental data in the whole temperature range.[17] Although it is difficult to refine every parameter to a high correction through the multiparameter fitting procedure because of some parameters having the same effect upon the bulk magnetic behavior,[14b,18] reliable information can be obtained through its self-complemented procedure to fit both susceptibility data. The results of the best fit are shown in Figure 9 with $g = 2.38$, $J = -19.6$ cm^{-1}, $D = 24.0$ cm^{-1}, $\Theta = -5.88$ K, $\rho = 0.028$, and $R = 8.2 \times 10^{-5}$ [$R = \sum(\chi_{obsd} - \chi_{calcd})^2/\sum\chi_{obsd}^2$] for **3** and $g = 2.48$, $J = -21.5$ cm^{-1}, $D = 31.0$ cm^{-1}, $\Theta = -6.50$, $\rho = 0.009$, and $R = 1.5 \times 10^{-4}$ for **4**. The coupling constants of -19.6 cm^{-1} for **3** and -21.5 cm^{-1} for **4** show a stronger intramolecular antiferromagnetic interaction in both complexes.

The separations of the two Co(II) centers in the prismatic dications $[Co_2(L)_4X_2]^{2+}$ are 5.636 Å for **3** and 5.807 Å for **4**, indicating no direct exchange pathway between metal centers. Ligands L, which are the only connectors of two cobalt(II) centers in every dimeric cage, are unfavorable for electronic interactions needed for the efficient superexchange between paramagnetic metal centers, as confirmed by the magnetic studies on other complexes of L (Figure S3 in the Supporting Information).[11] Thus, the strong intramolecular antiferromagnetic interactions in both complexes are peculiar and very interesting. According to their structural features, the magnetic-exchange interactions are likely to be propagated via the encapsulated anions X. Although weakly contacting with two cobalt(II) centers, the encapsulated X can lead to a head-on overlap of the Co d_{z^2} orbitals and X p_z orbital with the Co−X−Co bridging angle of 180°. Such efficient overlap is probably responsible for the stronger intramolecular antiferromagnetic interactions observed. Notably, the J values for both complexes are similar, which is consistent with the same magnetic topology of cobalt(II) halide complexes. A slight increase of J for complex **4** (also observed by EPR) may arise from the distinct properties of Br^- with the comparatively larger atom radius and electronic delocalization. The slightly bigger average g values of 2.38 for **3** and 2.48 for **4** fall in the range of that of high-spin cobalt(II) compounds because of modest spin−orbital coupling. As predicted by the EPR spectra (seen above), the magnetic simulations provide larger D values for complexes **3** and **4**. These valves also observed in other binuclear cobalt(II) complexes correlate well with their structural features (greatly axial-elongated square-pyramidal or octahedral coordination geometry).[14b,19]

Conclusions. A new class of cobalt(II) halide complexes of flexible ligand L, varying from polymers **1** and **2** to tetragonal prisms **3** and **4**, has been prepared. The structural motifs are clearly tuned by solvents, by the labile coordination configuration of cobalt(II) centers, and especially by the various conformations of L. Remarkably, the cobalt(II) chloride compounds are very dependent on the temperature, showing interestingly solvent-assisted temperature-dependent dynamic formation from polymers to discrete cages. The formation of tetragonal-prismatic cages **3** and **4** may be templated by the encapsulated anions Cl^- and Br^-, respectively. Further solution studies show that the cage structures have considerable stability even in polar solvents such as methanol and DMF. The results of EPR and magnetism investigations disclose that there is observed intramolecular magnetic-exchange coupling between high-spin cobalt(II) centers in the cages **3** and **4**. The values for the intramolecular spin-coupling constant J were estimated to be -19.6 and -21.5 cm^{-1} for **3** and **4**, respectively. Such strong antiferromagnetic coupling arises from the head-on overlap of the magnetic Co d_{z^2} orbitals and the p_z orbitals of the encapsulated anions Cl^- and Br^-, suggesting that weak interactions between the host and guest have significant effects upon the structural motif as well as the properties of the hosts. Further sophisticated theoretical calculations will help to gain insight into the magnetic-superexchange interactions mediated by guest anions.

Experimental Section

General Remarks. All materials reagents and solvents were purchased from commercial sources and used as received. Elemental analyses were determined on an Elementary Vario ELIII elemental analyzer. IR spectra were measured as KBr pellets on a Nicolet Magna 750 FT-IR spectrometer in the range of 400−4000 cm^{-1}. ESI-MS was performed on a DECAX-30000 LCQ Deca XP ion trap mass spectrometer. Electronic absorption spectra were recorded using a double-beam Lambda 35 UV−vis spectrometer. EPR measurements were done on a Bruker E500 spectrometer equipped with an Oxford-900 liquid-helium cryostat and an ITC-503 temperature controller. The temperature-dependent magnetic measurements were determined on a Quantum Design SQUID-XL7 magnetometer.

Synthesis of $[Co(L)_2Cl_2]\cdot Me_2CO$ (1). A solution of L (0.550 g, 2.0 mmol) and methanol (50 mL) was carefully layered over a solution of $CoCl_2\cdot 6H_2O$ (0.240 g, 1.0 mmol) and acetone (50 mL) at room temperature of about 25 °C. A blue-green floccule was suspended in the solution in about 5 min and then transformed into orange block crystals of **1** (0.46 g, 0.62 mmol, 62%) in another 5 min. Anal. Calcd for $C_{29}H_{30}Cl_2CoN_4O_3S_4$: C, 47.03; H, 4.08; N, 7.56; S, 17.31. Found: C, 46.85; H, 4.00; N, 7.68; S, 17.35. IR (KBr): $\tilde{\nu}$ 3060 (w), 2972 (w), 2931 (w), 2888 (w), 1713 (s), 1591

(17) MAGMUN4.0 is available free of charge from http://www.ucs.mun.ca/~lthomp/index.html. It has been developed by Dr. Zhiqiang Xu (Memorial University), in conjunction with Dr. O. Waldmann (waldmann@mps.ohio-state.edu).

(18) De Munno, G.; Julve, M.; Lloret, F.; Faus, J.; Caneschi, A. *J. Chem. Soc., Dalton Trans.* **1994**, 1175.

(19) Brewer, G.; Sinn, E. *Inorg. Chem.* **1985**, *24*, 4580.

Table 2. Crystal Data and Structure Refinement for **1**−**4**

param	**1**	**2**	**3**	**4**
formula	$C_{29}H_{30}Cl_2CoN_4O_3S_4$	$C_{19}H_{26}Cl_2CoN_4O_3S_2$	$C_{61}H_{81}Cl_4Co_2N_9O_{12}S_8$	$C_{70}H_{94}Br_4Co_2N_{14}O_{12}S_8$
fw	740.64	552.39	1648.50	2017.57
temp (K)	130(2)	293(2)	293(2)	130(2)
cryst syst	orthorhombic	orthorhombic	monoclinic	monoclinic
space group	*Pbca*	*Pccn*	*C2/m*	$P2_1/c$
a (Å)	18.457(6)	9.9218(7)	21.668(3)	13.7222(8)
b (Å)	16.262(5)	13.1236(9)	15.8946(15)	15.4895(8)
c (Å)	21.388(6)	18.0166(16)	13.8390(15)	21.8774(14)
β (deg)	90.00(0)	90.00(0)	113.520(4)	113.740(1)
V (Å^3)	6420(3)	2345.9(3)	4370.3(9)	4278.0(4)
Z; ρ_{calcd} (g/cm^3)	8; 1.533	4; 1.564	2; 1.254	2; 1.566
μ (mm^{-1})	1.000	1.166	0.746	2.515
GOF	1.166	1.135	1.161	1.091
R1; wR2 [$I > 2\sigma(I)$]	0.0620; 0.1364	0.0341; 0.0777	0.0851; 0.2520	0.0395; 0.0938

(vs), 1530 (w), 1481 (s), 1416 (s), 1220 (m), 1065 (m), 807 (m), 723 (m), 499 (m) cm^{-1}.

Synthesis of Co(L)Cl$_2$(DMF)$_2$ (2). At 30 °C, slow diffusion of diethyl ether (30 mL) into the 5-mL blue DMF solution of fresh complex **1** (0.074 g, 0.1 mmol) for 2 weeks created red prismatic crystals of **2** (0.040 g, 0.072 mmol, 72%). Anal. Calcd for $C_{19}H_{26}Cl_2CoN_4O_3S_2$: C, 41.31; H, 4.74; N, 10.14; S, 11.61. Found: C, 41.27; H, 4.65; N, 10.31; S, 11.64. IR (KBr): $\tilde{\nu}$ 3049 (w), 2993 (w), 2937 (w), 2880 (w), 1710 (m), 1643 (vs), 1581 (s), 1478 (m), 1412 (m), 1366 (s), 1105 (m), 816 (m), 724 (s), 677 (m), 498 (w) cm^{-1}.

Syntheses of [Co$_2$(L)$_4$Cl$_2$]Cl$_2$·Et$_2$O·DMF·2MeOH·4H$_2$O (3). At 10 °C, slow diffusion of diethyl ether (30 mL) into the 5-mL blue DMF solution of fresh complex **1** (0.074 g, 0.1 mmol) first created green jelly and then changed into purple prismatic crystals of **3** (0.069 g, 0.042 mmol, 84%) in 3 weeks. Anal. Calcd for $C_{61}H_{81}Cl_4Co_2N_9O_{12}S_8$: C, 44.44; H, 4.95; N, 7.65; S, 15.56. Found: C, 44.06; H, 4.81; N, 7.80; S, 15.62. IR (KBr): $\tilde{\nu}$ 3430 (w), 3055 (w), 2993 (w), 2937 (w), 2886 (w), 1715 (m), 1648 (vs), 1588 (s), 1540 (w), 1478 (m), 1412 (m), 1366 (s), 1104 (m), 816 (m), 718 (s), 498 (w) cm^{-1}.

Synthesis of [Co$_2$(L)$_4$Br$_2$]Br$_2$·6DMF·2H$_2$O (4). A solution of L (0.055 g, 0.2 mmol), $CoBr_2 \cdot 6H_2O$ (0.033 g, 0.1 mmol), and DMF (5 mL) was stirred for 1 h at room temperature. At 10 °C, slow diffusion of diethyl ether (30 mL) into the resultant blue solution for 3 weeks gave purple prismatic crystals of **4** (0.089 g, 0.044 mmol, 88%). Anal. Calcd for $C_{70}H_{94}Br_4Co_2N_{14}O_{12}S_8$: C, 41.67; H, 4.70; N, 9.72; S, 12.71. Found: C, 41.70; H, 4.64; N, 9.61; S, 12.57. IR (KBr): $\tilde{\nu}$ 3424 (m), 3055 (w), 2924 (w), 2889 (w), 1734 (w), 1658 (s), 1591 (vs), 1535 (w), 1488 (m), 1424 (m), 1226 (w), 1067 (w), 813 (w), 722 (m), 499 (w) cm^{-1}.

X-ray Structure Determinations. Single-crystal data were collected on a Rigaku mercury CCD diffractometer at 130 K for **1** and **4** and at room temperature for **2** and **3** using graphite-monochromated Mo Kα radiation ($\lambda = 0.7107$ Å). The structures were solved by direct methods and refined on F^2 by full-matrix least-squares procedures using the SHELXTL software suite.[20] All non-hydrogen atoms were refined anisotropically, and the hydrogen atoms were treated as idealized contributions except water molecules and those solvent molecules showing severe disorder in complex **3**. A summary of the crystallographic data of complexes **1**−**4** is listed in Table 2, and their selected bond lengths and angles are tabulated in Table 3.

Spectrophotometric Measurements. All operations were performed at room temperature (ca. 24 °C) using the UV−vis spectrometer described above. All solutions used to record UV−vis spectra were prepared in volumetric flasks. The reaction mixtures for spectrophotometric titrations prepared through retaining the original concentration of L (ca. 7.2×10^{-5}) were left to equilibrate before recording the spectra (equilibration was generally found to occur after 2 days).

Table 3. Selected Bond Lengths (Å) and Angles (deg) for **1**−**4**[a]

	Compound **1**		
Co1−N1	2.185(3)	Co1−N2A	2.184(3)
Co1−N3	2.180(3)	Co1−N4B	2.186(3)
Co1−Cl1	2.4106(12)	Co1−Cl2	2.4283(12)
N3−Co1−N1	88.60(13)	N2A-Co1−N1	90.17(13)
N3−Co1−N4B	92.15(13)	N2A-Co1−N4B	89.08(12)
N3−Co1−Cl1	89.78(9)	N2A-Co1−Cl1	90.01(9)
N1−Co1−Cl1	89.68(9)	N4B−Co1−Cl1	91.25(9)
N3−Co1−Cl2	90.69(9)	N2A-Co1−Cl2	89.50(9)
N1−Co1−Cl2	89.43(9)	N4B−Co1−Cl2	89.64(9)
N3−Co1−N2A	178.76(12)	N1−Co1−N4B	178.82(12)
Cl1−Co1−Cl2	178.98(4)		
	Compound **2**		
Co1−O1	2.1421(13)	Co1−N1	2.1932(15)
Co1−O1A	2.1421(13)	Co1−N1A	2.1932(15)
Co1−Cl1	2.4407(5)	Co1−Cl1A	2.4407(5)
O1−Co1−N1	91.52(6)	O1A−Co1−N1	88.48(6)
O1A−Co1−N1A	91.52(6)	O1−Co1−N1A	88.48(6)
O1A−Co1−Cl1A	90.50(4)	O1−Co1−Cl1A	89.50(4)
N1−Co1−Cl1A	90.49(4)	N1A−Co1−Cl1A	89.51(4)
O1A−Co1−Cl1	89.50(4)	O1−Co1−Cl1	90.50(4)
N1−Co1−Cl1	89.51(4)	N1A−Co1−Cl1	90.49(4)
O1A−Co1−O1	180.00(7)	N1−Co1−N1A	180.00(1)
Cl1A−Co1−Cl1	180.00(1)		
	Compound **3**		
Co1−N1	2.140(5)	Co1−N1A	2.140(5)
Co1−N2	2.159(5)	Co1−N2A	2.159(5)
Co1−Cl1	2.424(3)		
N1A−Co1−N2	91.64(18)	N1−Co1−N2A	91.64(18)
N1A−Co1−N2A	88.27(18)	N1−Co1−Cl1	93.22(14)
N1A−Co1−Cl1	93.22(14)	N2−Co1−Cl1	90.80(13)
N2A−Co1−Cl1	90.80(13)	N1−Co1−N2	88.27(18)
N1−Co1−N1A	173.6(3)	N2−Co1−N2A	178.4(3)
	Compound **4**		
Co1−N1	2.137(2)	Co1−N2A	2.138(2)
Co1−N3	2.159(2)	Co1−N4A	2.153(2)
Co1−Br1	2.6046(4)		
N1−Co1−N4A	93.18(8)	N2A−Co1−N4A	86.92(8)
N1−Co1−N3	89.15(8)	N2A−Co1−N3	90.48(8)
N1−Co1−Br1	91.86(6)	N2A−Co1−Br1	93.34(6)
N4A−Co1−Br1	90.59(6)	N3−Co1−Br1	92.49(5)
N1−Co1−N2A	174.80(8)	N4A−Co1−N3	176.08(8)

[a] Symmetry codes: A = $-x + {}^1/_2$, $-y$, $z + {}^1/_2$ and B = $x - {}^1/_2$, $-y + {}^3/_2$, $-z + 2$ for **1**; A = $-x$, $-y + 1$, $-z + 1$ for **2**; A = $-x + 1$, y, $-z + 1$ for **3**; A = $-x + 1$, $-y + 1$, $-z + 1$ for **4**.

Acknowledgment. This work was supported by grants of the National Nature Science Foundation of China and the

(20) Sheldrick, G. M. *SHELXTL-PC*; University of Göttingen, Göttingen, Germany, 1997.

Nature Science Foundation of Fujian Province. The EPR spectral measurements were completed by C.Z. The authors thank Dr. Xiaotai Wang for helpful suggestions.

Supporting Information Available: Crystallographic data in CIF format for **1**−**4**, ESI-MS spectra for complexes **1**·Me_2CO, **3**, and **4**, a selection of UV−vis spectra from the spectrophotometric titrations of L with $CoCl_2$ or $CoBr_2$ in methanol, and $1/\chi_M$ and χ_M vs *T* plots with the theoretical fit for **1**·Me_2CO and **2**. This material is available free of charge via the Internet at http://pubs.acs.org. Crystallographic data in CIF format have also been deposited with the Cambridge Crystallographic Data Centre, CCDC No. 261565-261568. Copies of this information may be obtained free of charge from the Director, CCDC, 12 Union Road, Cambridge CB2 1EZ, U.K. (fax +44-1223-336033; e-mail deposit@ccdc.cam.ac.uk; http://www.ccdc.cam.ac.uk).

IC050455V